

# Constraining $B$ -Mesogenesis models with inclusive and exclusive decays.

---

Alexander Lenz,<sup>a</sup> Ali Mohamed,<sup>a</sup> Zachary Wüthrich<sup>a</sup>

<sup>a</sup>*Physik Department, Universität Siegen, Walter-Flex-Str. 3, 57068 Siegen, Germany*

*E-mail:* [alexander.lenz@uni-siegen.de](mailto:alexander.lenz@uni-siegen.de), [Ali.Mohamed@uni-siegen.de](mailto:Ali.Mohamed@uni-siegen.de),  
[Zachary.Wuethrich@uni-siegen.de](mailto:Zachary.Wuethrich@uni-siegen.de)

ABSTRACT: The  $B$ -Mesogenesis model explains the matter-antimatter asymmetry and leads to the right amount of dark matter in the Universe. In particular, this model predicts new decay channels of the  $b$  quark. We investigate the modification of inclusive  $b$ -hadron decay rates and of the lifetimes of different  $B$  mesons due to these new decay channels and compare our results with available predictions for exclusive  $B$  meson decays. We find a small surviving parameter space where the  $B$ -Mesogenesis model is working and which has not been excluded by experiment. Experimental investigations in the near future should be able to test this remaining parameter space and thus either exclude or confirm the  $B$ -Mesogenesis model.

---

## Contents

<b>1</b>	<b>Introduction</b>	<b>1</b>
<b>2</b>	<b>The model</b>	<b>3</b>
<b>3</b>	<b>Contribution of the <math>B</math>-Mesogenesis model to flavour observables</b>	<b>4</b>
3.1	Inclusive decay rate	4
3.2	Exclusive decay rates	7
3.3	Lifetime differences	8
<b>4</b>	<b>Phenomenology</b>	<b>11</b>
4.1	Inclusive vs. exclusive decays	11
4.2	Lifetime ratios	12
<b>5</b>	<b>Summary</b>	<b>12</b>
<b>A</b>	<b>Numerical Inputs of the Constants <math>G_X^{f_1 f_2}</math></b>	<b>13</b>
<b>B</b>	<b>Supplementary plots</b>	<b>16</b>

---

## 1 Introduction

The Standard Model (SM) of particle physics is extremely successful in describing the microscopic world, it leaves, however, several fundamental questions unanswered, like the existence of matter in the Universe and the presence of dark matter. The  $B$ -Mesogenesis model discussed in Ref. [1] presents an interesting framework to solve both of these issues. In particular, this model predicts new decay channels of the  $b$ -quark into SM baryons and dark (i.e. invisible in particle physics detectors) anti-baryons. These new decay channels lead to new exclusive decay channels of  $b$  hadrons, as well as to a modification of inclusive decay channels and therefore of the lifetimes and to a modification of mixing observables.

For the new exclusive decay channels of  $b$  hadrons, theory predictions have been made recently within the framework of light cone sum rules [2, 3]:  $B^+$ -meson decays into a proton  $p^+$  and a dark antibaryon  $\bar{\psi}$ , i.e.  $B^+ \rightarrow p^+ \bar{\psi}$ , have been studied in Ref. [4] and higher twist corrections to this decay have been estimated in Ref. [5]. In these two works the  $B^+$  meson was described by an interpolating current, while the nucleon was described by its distribution amplitudes, which are known to higher twist [6–9].  $B$ -meson decays into different baryons  $\mathcal{B}$  (octet baryons or charmed anti-triplet baryon) and dark antibaryon,  $B^+ \rightarrow \mathcal{B} \bar{\psi}$ , were investigated in Ref. [10] using the leading twist distribution amplitudes of the different light baryons from Ref. [11]

and some simplifying assumptions for the charmed baryons. Finally, decays of heavy  $\Lambda_b$  and  $\Xi_b$  baryons into a pseudoscalar meson and a dark baryon were considered in Ref. [12], using the  $\Lambda_b$  distribution amplitudes obtained in Refs. [13, 14].

In this paper we will determine the full inclusive decay rate  $\Gamma(b \rightarrow d\nu\psi)$ <sup>1</sup>. To fulfill the requirement of the  $B$ -mesogenesis model, the corresponding inclusive branching fraction has to have a value of at least  $10^{-4}$ . By requiring this bound to be fulfilled, we will get lower bounds on the elementary  $b \rightarrow X\psi$  couplings, which can be inserted into the predictions of the exclusive decays in order to get lower bounds on the exclusive branching fraction, which are close to the experimental prospects for detecting these channels.

Lifetimes of  $b$  hadrons and lifetime ratios like  $\tau(B^+)/\tau(B_d)$  are by now experimentally known with a high precision [16]

$$\left(\frac{\tau(B^+)}{\tau(B_d)}\right)^{\text{Exp.}} = 1.076 \pm 0.004. \quad (1.1)$$

On the theoretical side, predictions for this ratio can be obtained within the framework of the heavy quark expansion (HQE), which has proven to be a powerful method to perform systematic studies of inclusive decay widths of heavy hadrons, see e.g. the reviews [17, 18]. Based on the calculations in Refs. [19–30], within the SM, the most recent value of the ratio reads [31]

$$\left(\frac{\tau(B^+)}{\tau(B_d)}\right)^{\text{HQE}} = 1.081^{+0.014}_{-0.016}, \quad (1.2)$$

in perfect agreement with the experimental measurements, albeit with larger uncertainties. In the presence of physics beyond the SM, new decay channels of the  $b$ -quark would also contribute to the total lifetime of the  $B$  meson, and consequently modify the lifetime ratio according to

$$\frac{\tau(B^+)^{\text{HQE}}}{\tau(B_d)} = 1 + [\Gamma^{\text{SM}}(B_d) - \Gamma^{\text{SM}}(B^+)] \tau^{\text{Exp.}}(B^+) + [\Gamma^{\text{BSM}}(B_d) - \Gamma^{\text{BSM}}(B^+)] \tau^{\text{Exp.}}(B^+), \quad (1.3)$$

so that, by comparing with the corresponding experimental determination, Eq. (1.3) can be used to constrain the favoured parameter space for a specific set of BSM operators. We determine the modification of the lifetime ratio due to the  $B$ -Mesogenesis model.

The new decay channels also modify mixing observables like the decay rate differences  $\Delta\Gamma_q$  and the semileptonic CP asymmetries  $a_{sl}^q$ , with  $q = d, s$ . Currently SM predictions for the mixing observables [24, 32–42] agree well with the experimental measurements, see e.g. HFLAV [16]. The modification of the mixing observables due to the  $B$ -Mesogenesis model have been recently determined in Ref. [43] and turned out to be small. Nevertheless a future more precise determination of the semileptonic CP asymmetries could have some impact on the  $B$ -Mesogenesis model.

The paper is organised as follows: in Section 2 we briefly summarize the new  $b$  quark decay channels within the  $B$ -Mesogenesis model. In Section 3 we describe the new contributions to

---

<sup>1</sup>Semi-inclusive decay rates were calculated in Ref. [15].

inclusive decay rates (Section 3.1), exclusive decay rates (Section 3.2) and the lifetime ratios (Section 3.2). The numerical study of the effects of the  $B$ -Mesogenesis model is described in Section 4. Finally, in Section 5 we summarise our results and give an outlook on future developments.

## 2 The model

The Baryogenesis model [1, 44] is based on  $B$  meson production in the early Universe, a process called " $B$ -Mesogenesis". The starting point is the assumption that the early Universe is dominated by a combination of radiation and a very weakly coupled scalar particle  $\Phi$ , which will decay into  $b\bar{b}$  pairs. The  $b$ -quarks then hadronize into  $B$  and  $\bar{B}$  meson pairs. In addition to standard decay channels, the  $B$  and  $\bar{B}$  mesons will subsequently decay through a new decay channel to visible baryons  $\mathcal{B}$  and dark anti-baryons  $\psi$ , which will appear as missing energy. Because of CP violation in the mixing of the neutral  $B_d$  and  $B_s$  systems,  $B_q$  and  $\bar{B}_q$  meson decays will result in different rates, generating the observed baryon asymmetry. Thus, this model not only directly relates the matter-antimatter imbalance to CP violation in the  $B$  system, but it also suggests a dark matter candidate, all originating from the  $B$  meson decays. For the decay  $B \rightarrow \psi\mathcal{B}$  to occur, a heavy color-triplet scalar mediator  $Y$  is introduced, which has baryon number  $-2/3$  and can carry  $-1/3$  or  $+2/3$  hypercharge. The most general renormalizable Lagrangian describing the interaction of a (hypercharge  $-1/3$  or  $2/3$ ) color-triplet scalar with quarks and the SM singlet baryon  $\psi$  is

$$\begin{aligned}\mathcal{L}_{-1/3} &= - \sum_{\alpha,\beta} y_{u_\alpha d_\beta} \epsilon_{ijk} Y^{*i} \bar{u}_{\alpha R}^j d_{\beta R}^{c,k} - \sum_{\gamma} y_{\psi d_\gamma} Y_i \bar{\psi} d_{\gamma R}^{c,i} + \text{h.c.}, \\ \mathcal{L}_{+2/3} &= - \sum_{\alpha,\beta} y_{d_\alpha d_\beta} \epsilon_{ijk} Y^{*i} \bar{d}_{\alpha R}^j d_{\beta R}^{c,k} - \sum_{\gamma} y_{\psi u_\gamma} Y_i \bar{\psi} u_{\gamma R}^{c,i} + \text{h.c.},\end{aligned}\tag{2.1}$$

where the  $y$ 's are the coupling constants, the subscripts  $i, j, k$  are the color indices,  $\alpha, \beta, \gamma$  denote the different flavours of the up and down quarks, and the superscript  $c$  is the charge conjugate operator. We use the convention that  $\psi_R^c = C^{-1} P_L^\top (\bar{\psi})^\top$  and  $\bar{\psi}_R^c = -\psi^\top P_R^\top C$ .

The Lagrangian in Eq. 2.1 will be used below to determine new contributions to inclusive  $B$  decays, to lifetimes of  $B$  mesons, and to exclusive  $B$  decays. The first step in this process is to integrate out the new heavy scalar and express the new physics in terms of four fermion operators. This process is diagrammatically shown in Figure 1. Note that the charge conjugation operator can be moved between fermions on the same fermion line, represented diagrammatically by reversing arrow directions and swapping hollow and filled in arrows. Following this procedure of integrating out the heavy scalar, and considering every possible diagram at tree level with the heavy scalar, we arrive at the set of effective vertices given in Figure 2.<sup>2</sup>

We can now easily reconstruct the necessary effective Hamiltonian to produce these effective vertices. In the case of the decay  $B^+ \rightarrow \psi p^+$  the relevant effective Hamiltonian is

---

<sup>2</sup>Throughout the paper, we neglect QCD corrections in the derivation of the effective Hamiltonian, treating them as a higher-order approximation.

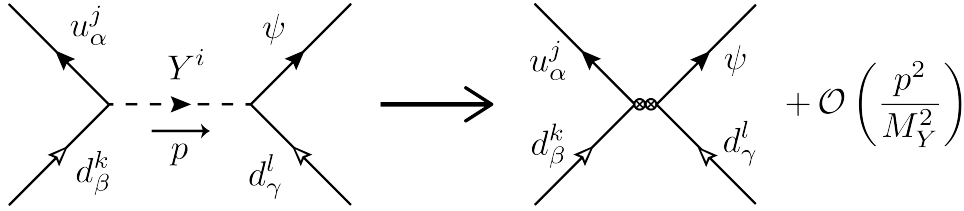


**Figure 1:** Diagrammatic representation of integrating out the heavy scalar degree of freedom. Hollow arrows represent charge conjugated fermions, while filled-in arrows represent non-charge conjugated fermions.

$$\mathcal{H}_{-1/3} = -\frac{y_{ub}y_{\psi d}}{M_Y^2} i\epsilon_{ijk} \bar{u}_R^i b_R^{c,j} \bar{d}_R^k \psi^c - \frac{y_{ub}^* y_{\psi d}^*}{M_Y^2} i\epsilon_{ijk} \bar{\psi}^c d_R^i \bar{b}_R^{c,j} u_R^k + \{b \leftrightarrow d\}, \quad (2.2)$$

which can be written as

$$\mathcal{H}_{-1/3} = -G_{(d)} \bar{\mathcal{O}}_{(d)} \psi^c - G_{(d)}^* \bar{\psi}^c \mathcal{O}_{(d)} + \{b \leftrightarrow d\}, \quad (2.3)$$

with the effective four-fermion coupling  $G_{(d)} = (y_{ub}y_{\psi d})/M_Y^2$ , and the local three-quark operators are defined as

$$\bar{\mathcal{O}}_{(d)} = i\epsilon_{ijk} (\bar{u}_R^i b_R^{c,j}) \bar{d}_R^k, \quad \mathcal{O}_{(d)} = i\epsilon_{ijk} d_R^i (\bar{b}_R^{c,j} u_R^k). \quad (2.4)$$

It is also possible for the  $b$ -quark to couple to the dark matter particle  $\psi$ , which leads to the following operators:

$$\bar{\mathcal{O}}_{(b)} = i\epsilon_{ijk} (\bar{u}_R^i d_R^{c,j}) \bar{b}_R^k, \quad \mathcal{O}_{(b)} = i\epsilon_{ijk} b_R^i (\bar{d}_R^{c,j} u_R^k). \quad (2.5)$$

For  $\mathcal{L}_{2/3}$ , the relevant part of the effective hamiltonian mediating the decay reads

$$\mathcal{H}_{2/3} = -G_{(u)} i\epsilon_{ijk} \bar{b}_R^i d_R^{c,j} \bar{\psi} u_R^{c,k} - G_{(u)}^* i\epsilon_{ijk} \bar{d}_R^{c,i} b_R^j \bar{u}_R^{c,k} \psi, \quad (2.6)$$

with the effective four-fermion coupling  $G_{(u)} = (y_{db}y_{\psi u})/M_Y^2$ .

For determining the lifetime ratios in Section 3.3, we will also include the four fermion operators involving two dark matter fields, or zero dark matter fields. However, these terms are irrelevant for the inclusive decay rate calculated in Section 3.1 and the exclusive decay rate calculated in Section 3.2.

### 3 Contribution of the $B$ -Mesogenesis model to flavour observables

#### 3.1 Inclusive decay rate

In order to predict the right amount of matter and dark matter in the Universe, the  $B$ -Mesogenesis model has to provide a certain minimal strength of the new decay channels [1]. This requirement is quantitatively encoded in a lower limit of the inclusive branching ratio of

$$= i \frac{y_{u_\alpha d_\beta}^* y_{u_\gamma d_\delta}}{M_Y^2} (\delta_{ik} \delta_{jl} - \delta_{il} \delta_{jk}) (CP_R \otimes P_L C^{-1})$$

$$= i \frac{y_{u_\alpha d_\beta} y_{\psi d_\gamma}}{M_Y^2} \epsilon_{ijk} (P_L C^{-1} \otimes P_L C^{-1})$$

$$= i \frac{y_{\psi d_\alpha} y_{\psi d_\beta}^*}{M_Y^2} N_c \delta_{ij} (CP_R \otimes P_L C^{-1})$$

(a) Effective vertices for  $\mathcal{L}_{-1/3}$ .

$$= i \frac{y_{d_\alpha d_\beta}^* y_{d_\gamma d_\delta}}{M_Y^2} (\delta_{ik} \delta_{jl} - \delta_{il} \delta_{jk}) (CP_R \otimes P_L C^{-1})$$

$$= i \frac{y_{d_\alpha d_\beta} y_{\psi u_\gamma}}{M_Y^2} \epsilon_{ijk} (P_L C^{-1} \otimes P_L C^{-1})$$

$$= i \frac{y_{\psi u_\alpha} y_{\psi u_\beta}^*}{M_Y^2} N_c \delta_{ij} (CP_R \otimes P_L C^{-1})$$

(b) Effective vertices for  $\mathcal{L}_{+2/3}$ .

**Figure 2:** Possible effective vertices arising from integrating out the heavy scalar. Conjugate diagrams are not shown. As each effective vertex must be inserted in two fermion lines, the  $(X \otimes Y)$  notation is meant to be interpreted as inserting  $X$  in the left fermion line, and inserting  $Y$  in the right fermion line (as seen in the diagram).

the  $B$  mesons into the dark baryon, i.e.  $\text{Br}(B \rightarrow \psi \mathcal{B} \mathcal{M}) > 10^{-4}$ , with a SM baryon  $\mathcal{B}$ , missing energy in the form of a dark sector antibaryon  $\psi$ , and any number of light mesons denoted by  $\mathcal{M}$ .

We calculate the LO-QCD term of the dimension 3 decay rate  $b \rightarrow du\psi$  in the framework of HQE. The corresponding Feynman diagrams are shown in Figure 3. Our starting point is exactly the effective Hamiltonian  $\mathcal{H}_{-1/3}$  in Eq. (2.3), which mediates this decay. Following [5], we consider the operators in Eqs. (2.4) and (2.5) as two individual versions of the  $B$ -Mesogenesis model and call them ( $d$ )- and ( $b$ )-model, respectively. This corresponds to the "type-2" and "type-1" operators in [1], where it is shown that the flavour constraints on the

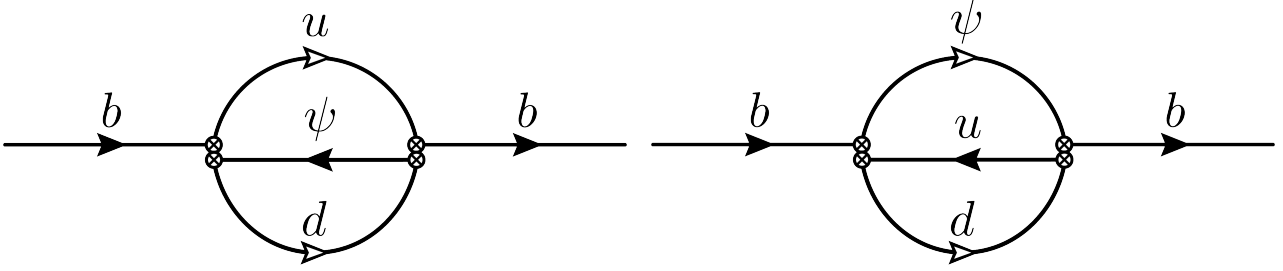


**Figure 3:** Diagrams contributing to the inclusive decay rate. Solid arrows indicate regular fermion lines, while hollow arrows indicate fermion lines involving the charge conjugation operator.

heavy color-triplet scalar  $Y$  imply that only one of the operators will be active and not a combination of both.<sup>3</sup>

By means of the optical theorem, the total decay width of a  $B$  meson can be related to the imaginary part of the forward-scattering matrix element of the time-ordered product of the double insertion of the effective Hamiltonian, i.e.

$$\Gamma(B) = \frac{1}{2m_B} \text{Im} \langle B | \mathcal{T} | B \rangle, \quad (3.1)$$

with the transition operator given by

$$\mathcal{T} = i \int d^4x T \{ \mathcal{H}_{\text{eff}}(x), \mathcal{H}_{\text{eff}}(0) \}. \quad (3.2)$$

The effective Hamiltonian  $\mathcal{H}_{\text{eff}}$  is given by the sum of the SM part and the  $B$  mesogenesis part

$$\mathcal{H}_{\text{eff}} = \mathcal{H}_{\text{eff}}^{\text{SM}} + \mathcal{H}_{-1/3}. \quad (3.3)$$

Within the HQE, the non-local operator in Eq. (3.2) can be expressed as a systematic expansion in inverse powers of the heavy  $b$ -quark mass, leading to the following series

$$\Gamma(B) = \Gamma_3 + \Gamma_5 \frac{\langle \mathcal{O}_5 \rangle}{m_b^2} + \Gamma_6 \frac{\langle \mathcal{O}_6 \rangle}{m_b^3} + \dots + 16\pi^2 \left( \tilde{\Gamma}_6 \frac{\langle \tilde{\mathcal{O}}_6 \rangle}{m_b^3} + \tilde{\Gamma}_7 \frac{\langle \tilde{\mathcal{O}}_7 \rangle}{m_b^4} + \dots \right), \quad (3.4)$$

where  $\Gamma_i$  are short-distance functions which can be computed perturbatively in QCD, and  $\langle \mathcal{O}_i \rangle \equiv \langle B | \mathcal{O}_i | B \rangle / (2m_B)$  denote the matrix element of local  $\Delta B = 0$  operators of increasing dimension  $i$ . For now we are only interested in the leading term  $\Gamma_3$ , which describes the free  $b$  quark decay. Below we will also consider higher order terms of Eq. (3.4) in order to investigate lifetime ratios of  $B$  mesons.

The LO-QCD contribution to the free quark decay of the channel  $b \rightarrow d u \psi$  reads

$$\begin{aligned} \Gamma_3^{(d)}(b \rightarrow d u \psi) &= \frac{|G_{(d)}|^2}{16} \frac{m_b^5}{192 \pi^3} [1 - 8\rho + 8\rho^3 - \rho^4 - 12\rho^2 \log(\rho)], \\ \Gamma_3^{(b)}(b \rightarrow d u \psi) &= \Gamma_3^{(d)}(b \rightarrow d u \psi) \Big|_{G_{(d)} \rightarrow G_{(b)}}, \end{aligned} \quad (3.5)$$

<sup>3</sup>It should be noted that there is a third operator version referred to as "type-3" in [1], where  $\psi$  is coupled to the up-type quarks. However, this appears in  $\mathcal{H}_{2/3}$ .

where  $\rho = m_\psi^2/m_b^2$ . We note, that this result is identical to the muon decay if we make the replacements  $|G_{(d)}|^2/16 \rightarrow G_F^2$ ,  $m_b \rightarrow m_\mu$  and  $m_\psi \rightarrow m_e$ . We observe that as the mass of the dark particle increases, the available phase space for the decay products of the  $B$ -meson becomes progressively smaller, vanishing at  $m_{B^+} - m_p = 4341.14$  MeV. We expect the inclusive approach to hold at masses considerably lower than that bound. In our analysis the region below 3 GeV will be most relevant.

For completeness, we also mention the result for  $\mathcal{H}_{2/3}$  and we find the result of the inclusive decay to be equal to Eq. (3.5) with the replacement

$$\Gamma_3^{(2/3)}(b \rightarrow d u \psi) = \Gamma_3^{(d)}(b \rightarrow d u \psi) \Big|_{G_{(d)} \rightarrow G_{(u)}}. \quad (3.6)$$

### 3.2 Exclusive decay rates

The exclusive decay for the channel  $B \rightarrow p^+ \psi$  was calculated for  $\mathcal{H}_{-1/3}$  in Ref. [5] using QCD light-cone sum rules up to twist six<sup>4</sup>. The exclusive decay width reads

$$\begin{aligned} \Gamma_{(d)}(B^+ \rightarrow p \psi) = & |G_{(d)}|^2 \left\{ \left[ \left( F_{B \rightarrow pR}^{(d)}(m_\psi^2) \right)^2 + \frac{m_\psi^2}{m_p^2} \left( \tilde{F}_{B \rightarrow pL}^{(d)}(m_\psi^2) \right)^2 \right] \right. \\ & \left. \times (m_B^2 - m_p^2 - m_\psi^2) + 2m_\psi^2 F_{B \rightarrow pR}^{(d)}(m_\psi^2) \tilde{F}_{B \rightarrow pL}^{(d)}(m_\psi^2) \right\} \frac{\lambda^{1/2}(m_B^2, m_p^2, m_\psi^2)}{16\pi m_B^3}, \end{aligned} \quad (3.7)$$

where  $F_{B \rightarrow pR}^{(d)}(q^2)$  and  $\tilde{F}_{B \rightarrow pL}^{(d)}(q^2)$  are the form factors

$$F_{B \rightarrow pR}^{(d)}(q^2) = \frac{F_{B \rightarrow pR}^{(d)}(0)}{1 - q^2/m_{\Lambda_b}^2} \left[ 1 + b_{B \rightarrow pR}^{(d)} \left( z(q^2) - z(0) + \frac{1}{2} [z(q^2)^2 - z(0)^2] \right) \right], \quad (3.8)$$

and  $\tilde{F}_{B \rightarrow pL}^{(d)}(q^2)$  is obtained by the replacement  $F_{B \rightarrow pR}^{(d)}(q^2) \rightarrow \tilde{F}_{B \rightarrow pL}^{(d)}(q^2)$ . Moreover

$$z(q^2) = (\sqrt{t_+ - q^2} - \sqrt{t_+ - t_0}) / (\sqrt{t_+ - q^2} + \sqrt{t_+ - t_0}), \quad (3.9)$$

with  $t_0 = (m_B + m_p) \cdot (\sqrt{m_B} - \sqrt{m_p})^2$  and  $t_\pm = (m_B \pm m_p)^2$ , where  $m_B$ ,  $m_p$  and  $m_{\Lambda_b}$  are the masses of the  $B$  meson, the proton and the  $\Lambda_b$  baryon, respectively.  $\lambda(x, y, z) = x^2 + y^2 + z^2 - 2xy - 2xz - 2yz$  is the Källén function, and  $b_{B \rightarrow pR}^{(d)}$  is the slope parameter obtained from the fitting procedures, for more details see [5]. The corresponding relation for the model (b) is obtained by a simple exchange of (d) with (b). The numerical values of the various parameters are listed in Table 1. We see that these decay rates are also proportional to  $|G_{(d)}|^2$  or  $|G_{(b)}|^2$ .

Therefore we start with the necessary bound on the inclusive branching ratio for the  $B$  mesogenesis model to work [1]

$$\begin{aligned} Br(B^+ \rightarrow \psi \mathcal{BM}) &> 10^{-4}, \\ Br(B^+ \rightarrow p^+ \psi) &> 10^{-4} \frac{\Gamma(B^+ \rightarrow p^+ \psi)}{\Gamma(B^+ \rightarrow \psi \mathcal{BM})} \equiv 10^{-4} \frac{\Gamma(B^+ \rightarrow p^+ \psi)}{\Gamma(b \rightarrow d u \psi)} \end{aligned} \quad (3.10)$$

<sup>4</sup>An exclusive decay analysis based on  $\mathcal{H}_{2/3}$  has not yet been performed.



Parameter	interval	Ref.
$b$ -quark $\overline{\text{MS}}$ mass	$\overline{m}_b(3 \text{ GeV}) = 4.47^{+0.04}_{-0.03} \text{ GeV}$	[45]
Form Factors	$F_{B \rightarrow p_R}^{(d)}(0) = 0.022^{+0.013}_{-0.013} \text{ GeV}^2$ $\tilde{F}_{B \rightarrow p_L}^{(d)}(0) = 0.005^{+0.002}_{-0.001} \text{ GeV}^2$ $F_{B \rightarrow p_R}^{(b)}(0) = -0.041^{+0.019}_{-0.018} \text{ GeV}^2$ $\tilde{F}_{B \rightarrow p_L}^{(b)}(0) = -0.007^{+0.003}_{-0.002} \text{ GeV}^2$	[5]
Slope parameters	$b_{B \rightarrow p_R}^{(d)} = 4.46^{+0.97}_{-1.72} \text{ GeV}^2$ $b_{B \rightarrow p_L}^{(d)} = -2.27^{+0.10}_{-0.08} \text{ GeV}^2$ $b_{B \rightarrow p_R}^{(b)} = -2.00^{+1.58}_{-3.62} \text{ GeV}^2$ $b_{B \rightarrow p_L}^{(b)} = -2.85^{+0.17}_{-0.15} \text{ GeV}^2$	[5]

**Table 1:** Input parameters in the LCSRs from the references in this Table.

to get a lower bound on the decay channel  $B^+ \rightarrow p^+ \psi$ . In the ratio of the decay rates in the last line of Eq. (3.10) the unknown couplings  $|G_{(d)}|^2$  or  $|G_{(b)}|^2$  cancel.

### 3.3 Lifetime differences

Finally we study the implications of the new decay channels of the  $b$ -quarks to the lifetime ratio  $\tau(B^+)/\tau(B_d)$ . For this quantity all 2-quark contributions in Eq. (3.4), i.e. the terms proportional to  $\langle \mathcal{O}_5 \rangle$ , are cancelling in the differences in Eq. (1.3) due to isospin symmetry. Thus in Eq. (1.3) only four-quark operator contributions survive starting from dimension-six, originating from loop-enhanced diagrams, as reflected by the explicit factor of  $16\pi^2$  in Eq. (3.4).<sup>5</sup> More details on the structure of the HQE for the  $b$ -system, as well as a complete list of references can be found e.g. in Ref. [29].

The leading (dimension-six and LO-QCD) contribution of the new decay channels in the imaginary part of the transition operator in Eq. (3.2) can be compactly written as

$$\text{Im} \mathcal{T}_{X,\text{NP}}^{f_1 f_2} = \frac{2m_b^2 G_X^{f_1 f_2} \sqrt{\lambda_{f_1 f_2}}}{192\pi} \left[ \sum_{n=1}^4 A_{X,n}^{f_1 f_2} \tilde{O}_n \right]. \quad (3.11)$$

<sup>5</sup>In fact, this is not the case for the lifetime ratio  $\tau(B_s)/\tau(B_d)$ , where  $\text{SU}(3)_F$  breaking effects play a dominant role. Therefore, a detailed study of BSM contributions to  $\tau(B_s)/\tau(B_d)$  would currently be strongly limited by the size of the non-perturbative input which parametrise the matrix elements of two-quark operators, and even more of the corresponding  $\text{SU}(3)_F$  breaking effects, which are poorly known, particularly for the Darwin operator, see e.g. the recent work [29]. Hence, given the current status of the SM prediction, we postpone the study of NP effects in  $\tau(B_s)/\tau(B_d)$  to a future work, once further insights on the size of matrix element of the Darwin operator and of the  $\text{SU}(3)_F$  breaking effects will become available.

Here  $X$  labels the topology (see Figure 4), while  $f_1$  and  $f_2$ , are the internal particles running in the loop, i.e. the light quarks or the dark matter particle  $\psi$ . The constants  $G_X^{f_1 f_2}$  are defined in Tables 2 and 3 in Appendix A for each topology and  $\lambda_{f_1 f_2} = (1 - r_{f_1} - r_{f_2})^2 - 4r_{f_1} r_{f_2}$ , with  $r_f = m_f^2/m_b^2$ . We also define the parameter  $\tilde{\lambda}_{f_1 f_2} \equiv 2(r_{f_1} - r_{f_2})^2 - (1 + r_{f_1} + r_{f_2})$ . The functions  $A_{X,n}^{f_1 f_2}$  in Eq. (3.11) are then linear combinations of the parameters  $\lambda_{f_1 f_2}$  and  $\tilde{\lambda}_{f_1 f_2}$ . The  $\Delta B = 0$  four-quark operators  $\tilde{O}_n$  are defined as

$$\tilde{Q}_1 = (\bar{q}^i \gamma_\mu P_R b^i)(\bar{b}^j \gamma^\mu P_R q^j), \quad \tilde{Q}_3 = (\bar{q}^i \gamma_\mu P_R t_{ij}^a b^j)(\bar{b}^r \gamma^\mu P_R t_{rm}^a q^m), \quad (3.12)$$

$$\tilde{Q}_2 = (\bar{q}^i P_L b^i)(\bar{b}^j P_R q^j), \quad \tilde{Q}_4 = (\bar{q}^i P_L t_{ij}^a b^j)(\bar{b}^r P_R t_{rm}^a q^m). \quad (3.13)$$

where  $q$  is  $u(d)$  for  $\Gamma(B_d)$  ( $\Gamma(B^+)$ ). It is worth noting that due to the fact that the values of the constants  $G_X^{f_1 f_2}$  corresponding to topologies where  $f_1, f_2 \neq \psi$  are extremely suppressed, the contributions of diagrams with both a BSM vertex and a SM vertex are negligible.

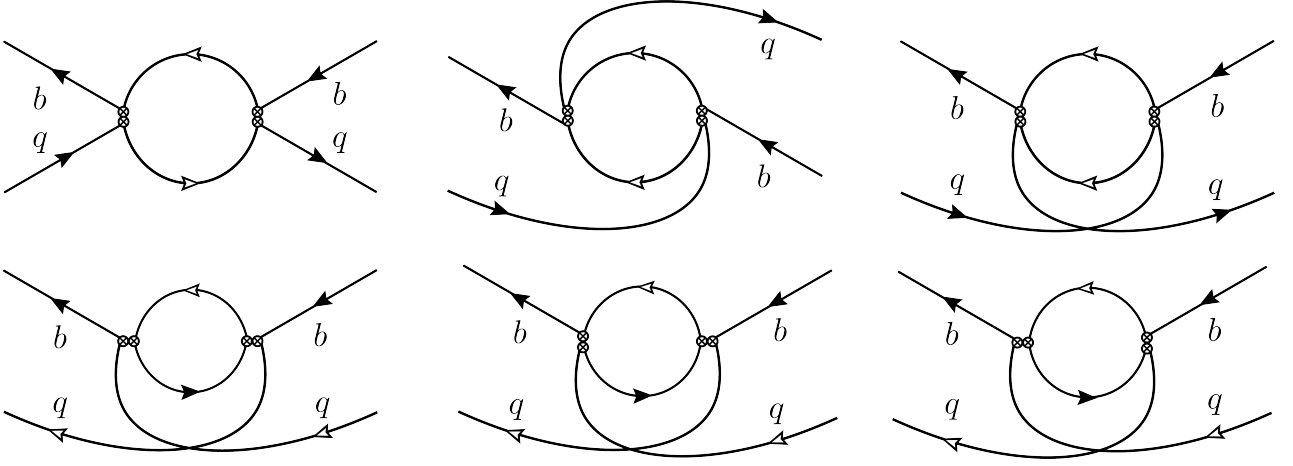


**Figure 4:** All the possible topologies that can show up in Eq. (3.11). From left to right, the top row corresponds to topologies  $I$ ,  $II$ , and  $III$  respectively and the bottom row corresponds to topologies  $IV$ ,  $V$ , and  $VI$  respectively. The possible internal fermions in the loop for each diagram depend on the specific effective vertices used. The list of possible effective vertices is provided in Figure 2.

### 3.3.1 Results for $\mathcal{H}_{-1/3}$

For  $\Gamma(B_d)$ , the analytic expressions for the entries  $A_{X,n}^{f_1 f_2}$  in Eq. (3.11) read

$$A_{III,1}^{\psi c} = \frac{2}{3}(-\lambda_{\psi c} + \tilde{\lambda}_{\psi c}), \quad A_{III,2}^{\psi c} = \frac{-4}{3}\tilde{\lambda}_{\psi c}, \quad A_{III,3}^{\psi c} = -3A_{III,1}^{\psi c}, \quad A_{III,4}^{\psi c} = -3A_{III,2}^{\psi c}, \quad (3.14)$$

$$A_{II,1}^{\psi c} = \frac{2}{3}\lambda_{\psi c}, \quad A_{II,2}^{\psi c} = \frac{-4}{3}\tilde{\lambda}_{\psi c}, \quad A_{II,3}^{\psi c} = -3A_{II,1}^{\psi c}, \quad A_{II,4}^{\psi c} = -3A_{II,2}^{\psi c}, \quad (3.15)$$

$$A_{I,1}^{\psi\psi} = -(\lambda_{\psi\psi} - \tilde{\lambda}_{\psi\psi}), \quad A_{I,2}^{\psi\psi} = -2\tilde{\lambda}_{\psi\psi}, \quad A_{I,3}^{\psi\psi} = A_{I,4}^{\psi\psi} = 0, \quad (3.16)$$

$$A_{I,1}^{cc} = -\frac{4}{3}(\lambda_{cc} - \tilde{\lambda}_{cc}), \quad A_{I,2}^{cc} = -\frac{8}{3}\tilde{\lambda}_{cc}, \quad A_{I,3}^{cc} = \frac{3}{2}A_{I,1}^{cc}, \quad A_{I,4}^{cc} = \frac{3}{2}A_{I,2}^{cc}, \quad (3.17)$$

while the remaining coefficient functions are obtained as follows

$$A_{X,n}^{f_1 f_2} = A_{X,n}^{f_2 f_1}, \quad A_{X,n}^{f_1 f_3} = A_{X,n}^{f_1 f_2} \Big|_{\lambda_{f_1 f_2}, \tilde{\lambda}_{f_1 f_2}, r_{f_2} \rightarrow \lambda_{f_1 f_3}, \tilde{\lambda}_{f_1 f_3}, r_{f_3}} \quad (3.18)$$

In the case of  $\Gamma(B^+)$ , the corresponding analytic expressions for  $A_{X,n}^{f_1 f_2}$  in Eq. (3.11) read

$$A_{IV,1}^{s\psi} = \frac{-8}{3}\lambda_{s\psi} + \frac{4}{3}\tilde{\lambda}_{s\psi}, \quad A_{IV,2}^{s\psi} = 0, \quad A_{IV,3}^{s\psi} = -3A_{IV,1}^{s\psi}, \quad A_{IV,4}^{s\psi} = 0, \quad (3.19)$$

$$A_{III,1}^{\psi s} = \frac{-2}{3}\lambda_{\psi s} + \frac{2}{3}\tilde{\lambda}_{\psi s}, \quad A_{III,2}^{\psi s} = \frac{-4}{3}\tilde{\lambda}_{\psi s}, \quad A_{III,3}^{\psi s} = -3A_{III,1}^{\psi s}, \quad A_{III,4}^{\psi s} = -3A_{III,2}^{\psi s} \quad (3.20)$$

$$A_{V,1}^{s\psi} = \frac{8}{6}\lambda_{s\psi} - \frac{4}{6}\tilde{\lambda}_{s\psi}, \quad A_{V,2}^{s\psi} = 0, \quad A_{V,3}^{s\psi} = \frac{-6}{2}A_{V,1}^{s\psi}, \quad A_{V,4}^{s\psi} = 0, \quad (3.21)$$

$$A_{VI,n}^{s\psi} = A_{V,n}^{s\psi}, \quad (3.22)$$

$$A_{IV,1}^{sc} = -\frac{2}{3}(8\lambda_{sc} - 4\tilde{\lambda}_{sc}), \quad A_{IV,2}^{sc} = 0, \quad A_{IV,3}^{sc} = -3A_{IV,1}^{sc}, \quad A_{IV,4}^{sc} = 0, \quad (3.23)$$

$$A_{I,1}^{sc} = -\frac{8}{6}(\lambda_{sc} - \tilde{\lambda}_{sc}), \quad A_{I,2}^{sc} = -\frac{8}{3}\tilde{\lambda}_{sc}, \quad A_{I,3}^{sc} = \frac{3}{2}A_{I,1}^{sc}, \quad A_{I,4}^{sc} = \frac{3}{2}A_{I,2}^{sc}, \quad (3.24)$$

The remaining functions are obtained from the following replacement

$$A_{X,n}^{f_1 f_3} = A_{X,n}^{f_1 f_2} \Big|_{\lambda_{f_1 f_2}, \tilde{\lambda}_{f_1 f_2}, r_{f_2} \rightarrow \lambda_{f_1 f_3}, \tilde{\lambda}_{f_1 f_3}, r_{f_3}}. \quad (3.25)$$

### 3.3.2 Results for $\mathcal{H}_{2/3}$

For  $\Gamma(B_d)$ , the analytic expressions for the entries  $A_{X,n}^{f_1 f_2}$  in Eq. (3.11) read

$$A_{IV,1}^{\psi c} = \frac{2}{3}(-4\lambda_{\psi c} + 2\tilde{\lambda}_{\psi c}), \quad A_{IV,3}^{\psi c} = -3A_{IV,1}^{\psi c}, \quad A_{IV,2}^{\psi c} = A_{IV,4}^{\psi c} = 0, \quad (3.26)$$

$$A_{IV,1}^{ds} = \frac{-2}{3}(8\lambda_{ds} - 4\tilde{\lambda}_{ds}), \quad A_{IV,3}^{ds} = -3A_{IV,1}^{ds}, \quad A_{IV,2}^{ds} = A_{IV,4}^{ds} = 0, \quad (3.27)$$

$$A_{I,1}^{ss} = \frac{-8}{6}(\lambda_{ss} + \tilde{\lambda}_{ss}), \quad A_{I,2}^{ss} = \frac{16}{6}\tilde{\lambda}_{ss}, \quad A_{I,3}^{ss} = \frac{3}{2}A_{I,1}^{ss}, \quad A_{I,4}^{ss} = \frac{3}{2}A_{I,2}^{ss}, \quad (3.28)$$

while the remaining coefficient functions are obtained as follows

$$A_{IV,n}^{\psi u} = A_{IV,n}^{\psi c} \Big|_{\lambda_{\psi c}, \tilde{\lambda}_{\psi c}, r_c \rightarrow \lambda_{\psi u}, \tilde{\lambda}_{\psi u}, r_u}, \quad A_{I,n}^{sd} = A_{I,n}^{ss} \Big|_{\lambda_{ss}, \tilde{\lambda}_{ss}, r_s \rightarrow \lambda_{sd}, \tilde{\lambda}_{sd}, r_d}. \quad (3.29)$$

In the case of  $\Gamma(B^+)$ , the corresponding analytic expressions for  $A_{X,n}^{f_1 f_2}$  in Eq. (3.11) read

$$A_{III,1}^{s\psi} = \frac{-2}{3}(\lambda_{s\psi} - \tilde{\lambda}_{s\psi}), \quad A_{III,2}^{s\psi} = \frac{-4}{3}\tilde{\lambda}_{s\psi}, \quad A_{III,3}^{s\psi} = -3A_{III,1}^{s\psi}, \quad A_{III,4}^{s\psi} = -3A_{III,2}^{s\psi} \quad (3.30)$$

The remaining functions are obtained from the following replacement

$$A_{III,n}^{d\psi} = A_{III,n}^{s\psi} \Big|_{\lambda_{s\psi}, \tilde{\lambda}_{s\psi}, r_s \rightarrow \lambda_{d\psi}, \tilde{\lambda}_{d\psi}, r_d}. \quad (3.31)$$

### 3.3.3 Matrix elements of four quark operators

We discuss now the parametrisation of the matrix element of the  $\Delta B = 0$  four-quark operators. The new operators arising in Eq. (3.12) and Eq. (3.13) differ from the SM ones only by a chirality transformation and therefore their matrix elements yield the same results as in the SM. We stress that in order to be consistent with the SM prediction of  $\tau(B^+)/\tau(B_d)$ , obtained in Ref. [31], and which we use in our analysis, we also parametrise the operators in HQET. In fact, any difference between operators defined in QCD or HQET arises only at dimension-seven, which we do not include in the present work. We thus have

$$\langle B | \tilde{\mathcal{O}}_n | B \rangle = f_B^2 m_B^2 \mathcal{B}_n, \quad (3.32)$$

where  $f_B$  is the QCD decay constant, and  $\mathcal{B}_n$  denote the corresponding Bag parameters. Within vacuum insertion approximation (VIA), it is easy to show that

$$\mathcal{B}_1 = \mathcal{B}_2 = 1, \quad \mathcal{B}_3 = \mathcal{B}_4 = 0. \quad (3.33)$$

We emphasise that for the Bag parameters  $\mathcal{B}_i$ , with  $i = 1, \dots, 4$ , also computations based on HQET sum rule are available [19, 24, 30], however, the deviation from their VIA values is found to be small, at most of the order of few percents. In our numerical analysis, we use for  $\mathcal{B}_i$ , with  $i = 1, \dots, 4$ , the determination from Ref. [19].

## 4 Phenomenology

### 4.1 Inclusive vs. exclusive decays

First we study the lower limit on the exclusive decay  $\Gamma_{\text{exl}}(B \rightarrow p^+ \psi)$  obtained in Eq. (3.10) as a function of the mass of the dark matter particle  $m_\psi$  in Figure 5. Note that the unknown couplings  $G_{(d,b)}$  are cancelling. In estimating the theory uncertainties, we follow two approaches. The first approach is a conservative scenario where we consider the maximal deviation of the prediction from the central values, when varying all input parameter in the region given in Table 1. The second approach is adding the uncertainties in quadrature, and this results in similar overall uncertainties.

In an attempt to search for direct evidence of the  $B$ -Mesogenesis model, the BABAR Collaboration conducted a study of the decay  $B^+ \rightarrow \psi p^+$  [46]. Although no direct signal was observed, they established an upper bound on the branching ratio  $\text{Br}(B^+ \rightarrow \psi p^+)$ , as illustrated in Figure 5.

For the  $B$ -Mesogenesis model to be valid the branching fraction of the  $B^+ \rightarrow p^+ \psi$  decay has to be above the red dotted line. Experimentally branching fractions of this decay inside the blue area have already been excluded. The the remaining allowed region is given in white and indicates that masses for the dark matter particle  $\psi$  above 3 GeV are excluded. For masses below 3 GeV there is still some possibility for the  $B$ -Mesogenesis model to work, which can, however, be tested by future, more precise experimental studies.

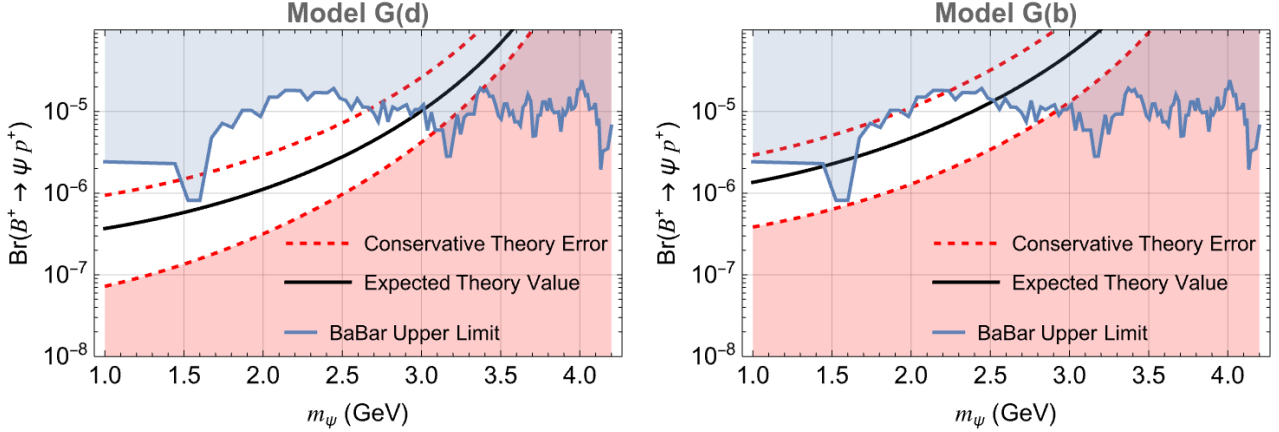


**Figure 5:** The red shaded region corresponds to the excluded region if one assumes the  $B$  mesogenesis model to work. The blue shaded region corresponds to the 90% CL excluded region from the BABAR upper limit of  $\text{Br}(B^+ \rightarrow p^+\psi)$ . The remaining allowed region is given in white.

## 4.2 Lifetime ratios

Next we investigate the impact of the  $B$ -Mesogenesis model on the lifetime ratio  $\tau(B^+)/\tau(B_d)$ . To constrain the numerical values of the parameters of the  $B$ -Mesogenesis model, we note that the studies in [1] have shown that ATLAS and CMS searches for color-triplet scalar impose stringent constraints on the constants  $G_X^{f_1 f_2}$ . We use the maximum values of these constants listed in Tables 2 and 3 to plot the lifetime ratio as a function of the mass of the dark sector particle  $\psi$ , as shown in Figures 6, 7 and 8 in Appendix B. There we have turned on one constant at a time, while all others are turned off. Unfortunately we find that within uncertainties the theory prediction overlaps always with the experimental value for all values of  $m_\psi$ . Hence we conclude that the study of the implications of the  $B$ -Mesogenesis model on the lifetime ratio  $\tau(B^+)/\tau(B_d)$  does not currently impose further constraints on the constants  $G_X^{f_1 f_2}$ .

## 5 Summary

By comparing the inclusive decay rate  $\Gamma(B^+ \rightarrow \psi \mathcal{B}\mathcal{M})$  to the exclusive decay rate  $\Gamma(B^+ \rightarrow p^+\psi)$  and taking their ratio, we obtained a lower bound for the branching ratio  $\text{Br}(B^+ \rightarrow p^+\psi)$  as a function of only the dark matter particle's mass  $m_\psi$ , independent of any arbitrary coupling constants. This lower bound excludes the possibility of the mass  $m_\psi$  being larger than 3 GeV given the most up to date upper bounds from BABAR, and motivates further experimental analysis of this decay as the remaining valid regions in parameter space are relatively small, and may be explored soon with future data, either confirming or excluding the  $B$ -Mesogenesis model.

Examining the lifetime ratios, we found the effect of the  $B$ -Mesogenesis scenario to be minimal, excluding the lifetime ratio as a discriminating observable for this model unless significant

improvements are made in the SM uncertainty.

Another future improvement of our analysis could be the determination of the exclusive decays with LCSR using the  $B$  meson distribution amplitude, instead of the nucleon distribution amplitude, as done so far.

## Acknowledgements

We thank Alexander Khodjamirian for many insightful discussions, a carefully reading of the manuscript and suggesting to study the ratio given in Eq. (3.10) and Miguel Escudero for helpful explanations related to the  $B$  mesogenesis model. A. M. and Z. W. would like to thank Maria Laura Piscopo and Aleksey Rusov for help with the first steps in the foundations of the heavy quark expansion and inclusive decays. Moreover, we would like to thank Anastasia Boushmelev for explaining the calculations and error analysis of the exclusive decays  $B^+ \rightarrow p^+\psi$  in Ref. [5].

This project was supported by the Deutsche Forschungsgemeinschaft (DFG, German Research Foundation) under grant 396021762-TRR 257 and the BMBF project ‘‘Theoretische Methoden f ur LHCb und Belle II’’ (F orderkennzeichen 05H21PSCLA/ErUM-FSP T04).

## A Numerical Inputs of the Constants $G_X^{f_1 f_2}$

In Tables 2 and 3, we define and list the maximum values for the constants  $G_X^{f_1 f_2}$  introduced in Eq. (3.11), as estimated in [1].

**Table 2:**  $\mathcal{H}_{-1/3}$  Constants and their Max values, taken from Ref. [1].

Parameter	Max Value (GeV) <sup>-4</sup>	Source
$G_{III}^{\psi u} = \frac{y_{ub}y_{\psi d}}{M_Y^2} \frac{y_{ub}^*y_{\psi d}^*}{M_Y^2}$	$1 \times 10^{-13}$	Table II
$G_{III}^{\psi c} = \frac{y_{cb}y_{\psi d}}{M_Y^2} \frac{y_{cb}^*y_{\psi d}^*}{M_Y^2}$	$1.5 \times 10^{-12}$	Table II
$G_{III}^{\psi b} = \frac{y_{ud}y_{\psi b}}{M_Y^2} \frac{y_{ud}^*y_{\psi b}^*}{M_Y^2}$	$4.7 \times 10^{-15}$	Table II
$G_{III}^{c\psi} = \frac{y_{cd}y_{\psi b}}{M_Y^2} \frac{y_{cd}^*y_{\psi b}^*}{M_Y^2}$	$1.6 \times 10^{-13}$	Table II
$G_{II}^{\psi u} = \frac{y_{ub}y_{\psi d}}{M_Y^2} \frac{y_{ud}^*y_{\psi b}^*}{M_Y^2}$	$2.2 \times 10^{-14}$	Table II
$G_{II}^{\psi c} = \frac{y_{cb}y_{\psi d}}{M_Y^2} \frac{y_{cd}^*y_{\psi b}^*}{M_Y^2}$	$4.9 \times 10^{-13}$	Table II
$G_{II}^{u\psi} = \frac{y_{ud}y_{\psi b}}{M_Y^2} \frac{y_{ub}^*y_{\psi d}^*}{M_Y^2}$	$2.2 \times 10^{-14}$	Table II

Continued on the next page

Table 2 – continued from previous page

Parameter	Max Value (GeV) <sup>-4</sup>	Source
$G_{II}^{c\psi} = \frac{y_{cd}y_{\psi b}}{M_Y^2} \frac{y_{cb}^*y_{\psi d}^*}{M_Y^2}$	$4.9 \times 10^{-13}$	Table II
$G_I^{\psi\psi} = \frac{y_{\psi d}y_{\psi b}^*}{M_Y^2} \frac{y_{\psi b}y_{\psi d}^*}{M_Y^2}$	$1.7 \times 10^{-15}$	Eq. (43j), Eq. (41a)
$G_I^{uu} = \frac{y_{ud}y_{ub}^*}{M_Y^2} \frac{y_{ub}y_{ud}^*}{M_Y^2}$	$1.7 \times 10^{-15}$	Eq. (43f), Eq. (41a)
$G_I^{cc} = \frac{y_{cd}y_{cb}^*}{M_Y^2} \frac{y_{cb}y_{cd}^*}{M_Y^2}$	$1.7 \times 10^{-15}$	Eq. (43f), Eq. (41a)
$G_I^{cu} = \frac{y_{ud}y_{cb}^*}{M_Y^2} \frac{y_{cb}y_{ud}^*}{M_Y^2}$	$8.5 \times 10^{-16}$	Eq. (43e), Eq. (41a)
$G_I^{uc} = \frac{y_{cd}y_{ub}^*}{M_Y^2} \frac{y_{ub}y_{cd}^*}{M_Y^2}$	$8.5 \times 10^{-16}$	Eq. (43e), Eq. (41a)
$G_{IV}^{s\psi} = \frac{y_{\psi s}y_{ub}}{M_Y^2} \frac{y_{ub}^*y_{\psi s}^*}{M_Y^2}$	$1 \times 10^{-13}$	Table II
$G_{IV}^{d\psi} = \frac{y_{\psi d}y_{ub}}{M_Y^2} \frac{y_{ub}^*y_{\psi d}^*}{M_Y^2}$	$1 \times 10^{-13}$	Table II
$G_{III}^{\psi s} = \frac{y_{\psi b}y_{us}}{M_Y^2} \frac{y_{us}^*y_{\psi b}^*}{M_Y^2}$	$3.7 \times 10^{-14}$	Table II
$G_{III}^{\psi d} = \frac{y_{\psi b}y_{ud}}{M_Y^2} \frac{y_{ud}^*y_{\psi b}^*}{M_Y^2}$	$4.7 \times 10^{-15}$	Table II
$G_V^{\psi s} = \frac{y_{\psi s}y_{ub}}{M_Y^2} \frac{y_{us}^*y_{\psi b}^*}{M_Y^2}$	$6.3 \times 10^{-14}$	Table II
$G_V^{\psi d} = \frac{y_{\psi d}y_{ub}}{M_Y^2} \frac{y_{ud}^*y_{\psi b}^*}{M_Y^2}$	$2.2 \times 10^{-14}$	Table II
$G_{VI}^{\psi s} = \frac{y_{\psi b}y_{us}}{M_Y^2} \frac{y_{ub}^*y_{\psi s}^*}{M_Y^2}$	$6.3 \times 10^{-14}$	Table II
$G_{VI}^{\psi d} = \frac{y_{\psi b}y_{ud}}{M_Y^2} \frac{y_{ub}^*y_{\psi d}^*}{M_Y^2}$	$2.2 \times 10^{-14}$	Table II
$G_{IV}^{cs} = \frac{y_{cs}y_{ub}^*}{M_Y^2} \frac{y_{ub}y_{cs}^*}{M_Y^2}$	$8.5 \times 10^{-15}$	Eq. (43g), Eq. (41a)
$G_{IV}^{us} = \frac{y_{us}y_{ub}^*}{M_Y^2} \frac{y_{ub}y_{us}^*}{M_Y^2}$	$8.5 \times 10^{-15}$	Eq. (43g), Eq. (41a)
$G_{IV}^{cd} = \frac{y_{cd}y_{ub}^*}{M_Y^2} \frac{y_{ub}y_{cd}^*}{M_Y^2}$	$8.5 \times 10^{-16}$	Eq. (43e), Eq. (41a)
$G_{IV}^{ud} = \frac{y_{ud}y_{ub}^*}{M_Y^2} \frac{y_{ub}y_{ud}^*}{M_Y^2}$	$1.7 \times 10^{-15}$	Eq. (43f), Eq. (41a)
$G_I^{cs} = \frac{y_{us}y_{cb}^*}{M_Y^2} \frac{y_{cb}y_{us}^*}{M_Y^2}$	$8.5 \times 10^{-15}$	Eq. (43g), Eq. (41a)
$G_I^{us} = \frac{y_{us}y_{ub}^*}{M_Y^2} \frac{y_{ub}y_{us}^*}{M_Y^2}$	$8.5 \times 10^{-15}$	Eq. (43g), Eq. (41a)

Continued on the next page

**Table 2** – continued from previous page

Parameter	Max Value (GeV) <sup>-4</sup>	Source
$G_I^{cd} = \frac{y_{ud}y_{cb}^* y_{cb}y_{ud}^*}{M_Y^2 M_Y^2}$	$8.5 \times 10^{-16}$	Eq. (43e), Eq. (41a)
$G_I^{ud} = \frac{y_{ud}y_{ub}^* y_{ub}y_{ud}^*}{M_Y^2 M_Y^2}$	$1.7 \times 10^{-15}$	Eq. (43f), Eq. (41a)

**Table 3:**  $\mathcal{H}_{2/3}$  Constants and their Max values, taken from Ref. [1].

Parameter	Max Value (GeV) <sup>-4</sup>	Source
$G_{IV}^{u\psi} = \frac{y_{bd}y_{\psi u} y_{bd}^*y_{\psi u}^*}{M_Y^2 M_Y^2}$	$2.5 \times 10^{-13}$	Table II
$G_{IV}^{c\psi} = \frac{y_{bd}y_{\psi c} y_{bd}^*y_{\psi c}^*}{M_Y^2 M_Y^2}$	$2.5 \times 10^{-13}$	Table II
$G_{IV}^{ds} = \frac{y_{ds}y_{bd}^* y_{bd}y_{ds}^*}{M_Y^2 M_Y^2}$	$8.5 \times 10^{-15}$	Eq. (44d), Eq. (41a)
$G_I^{ds} = \frac{y_{ds}y_{bd}^* y_{bd}y_{ds}^*}{M_Y^2 M_Y^2}$	$8.5 \times 10^{-15}$	Eq. (44d), Eq. (41a)
$G_I^{ss} = \frac{y_{ds}y_{bs}^* y_{bs}y_{ds}^*}{M_Y^2 M_Y^2}$	$1.7 \times 10^{-15}$	Eq. (44c), Eq. (41a)
$G_{III}^{d\psi} = \frac{y_{bd}y_{\psi u} y_{bd}^*y_{\psi u}^*}{M_Y^2 M_Y^2}$	$2.5 \times 10^{-13}$	Table II
$G_{III}^{s\psi} = \frac{y_{bs}y_{\psi u} y_{bs}^*y_{\psi u}^*}{M_Y^2 M_Y^2}$	$1.2 \times 10^{-12}$	Table II



## B Supplementary plots

In Figures 6 and 7, we show the lifetime ratio  $\tau(B^+)/\tau(B_d)$  as a function of the dark sector mass  $m_\psi$  when only one constant  $G_X^{f_1 f_2}$  is turned on to their maximum value and the others are set to zero. The maximum values for the different constants  $G_X^{f_1 f_2}$  are provided in Tables 2 and 3.

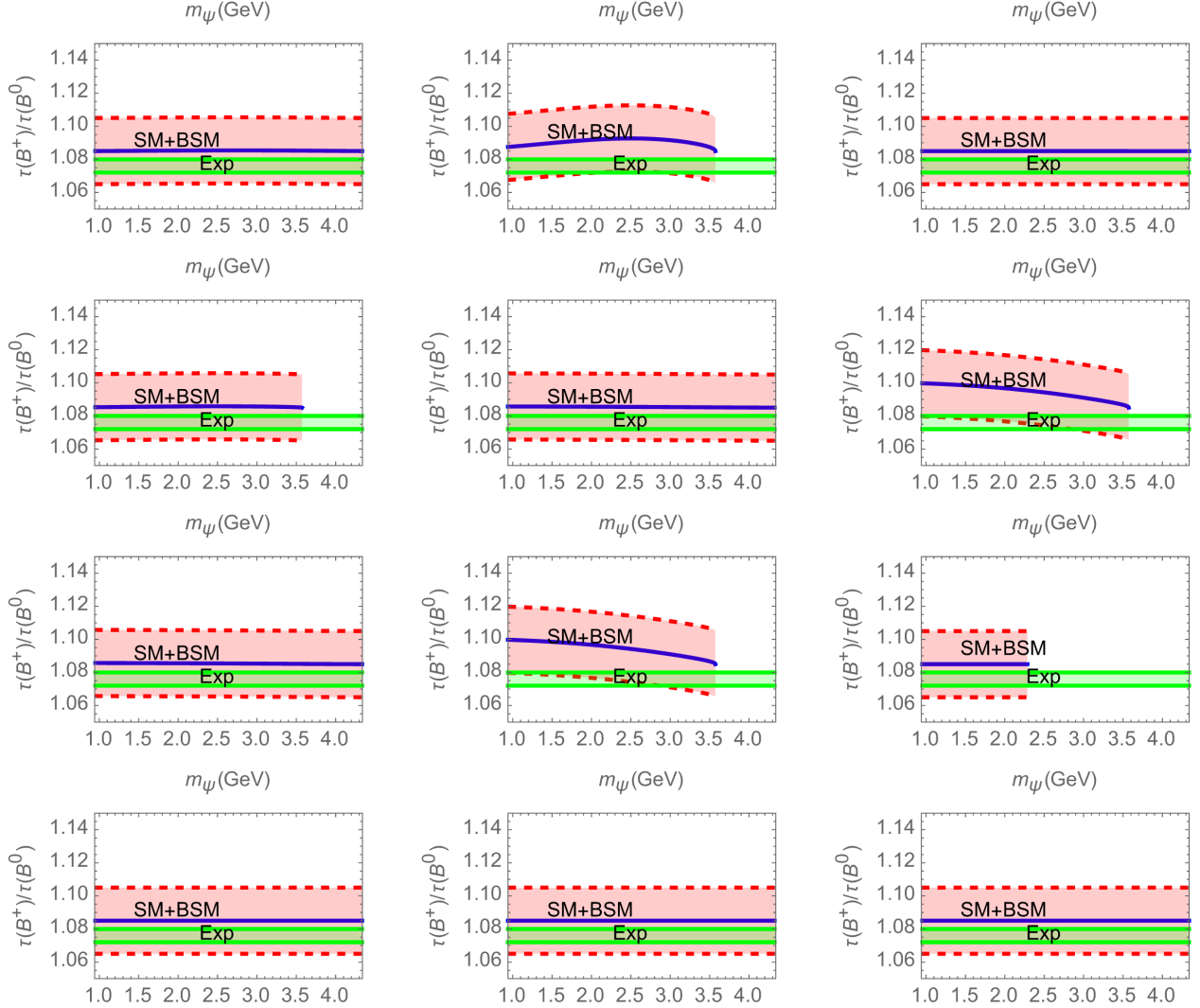


**Figure 6:** The lifetime ratio  $\tau(B^+)/\tau(B_d)$  for  $\mathcal{H}_{-1/3}$  as a function of  $m_\psi$ , using the upper limits of one the constants  $G_X^{q_1 q_2}$  and setting the others to zero. The red region shows the SM error, whereas the experimental value is shown in green. The non-vanishing constants from up to down and left to right are  $G_{III}^{\psi u}, G_{III}^{\psi c}, G_{III}^{u\psi}, G_{III}^{c\psi}, G_{II}^{\psi u}, G_{II}^{\psi c}, G_{II}^{u\psi}, G_{II}^{c\psi}, G_I^{\psi\psi}, G_I^{uu} = G_I^{cc}, G_I^{cu}, G_I^{uc}$

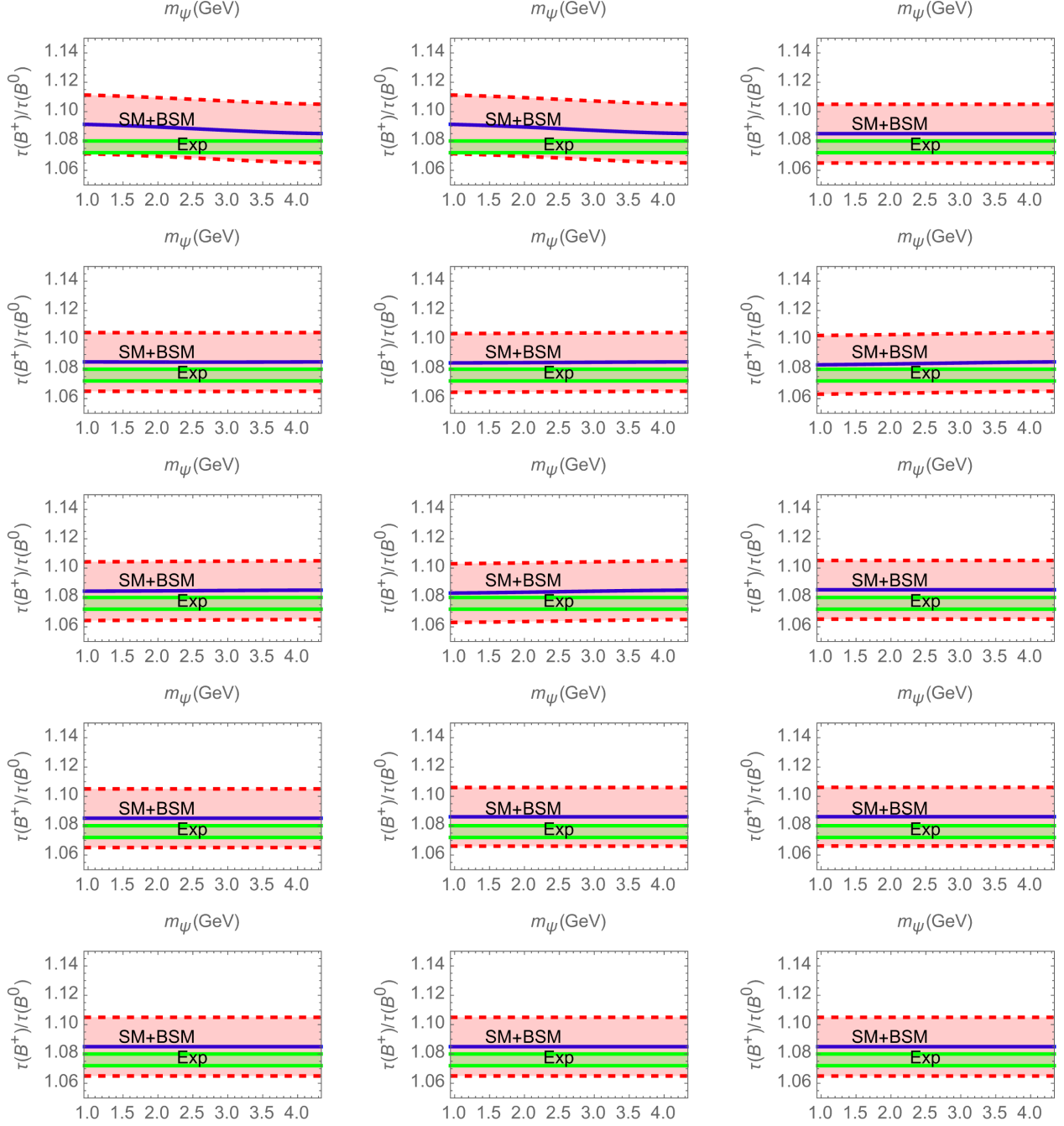


**Figure 7:** The lifetime ratio  $\tau(B^+)/\tau(B^0)$  for  $\mathcal{H}_{-1/3}$  as a function of  $m_\psi$ , using the upper limits of one of the constants  $G_X^{f_1 f_2}$  and setting the others to zero. The red region shows the SM error, whereas the experimental value is shown in green. The non-vanishing constants from up to down and left to right are  $G_{IV}^{\psi d}, G_{IV}^{\psi s}, G_{III}^{\psi d}, G_{III}^{\psi s}, G_V^{\psi d}, G_V^{\psi s}, G_{VI}^{\psi d}, G_{VI}^{\psi s}, G_{IV}^{rd}, G_{IV}^{cd}, G_I^{sc}, G_I^{su}, G_I^{du}, G_I^{dc}, G_I^{sc}, G_I^{su}$ .

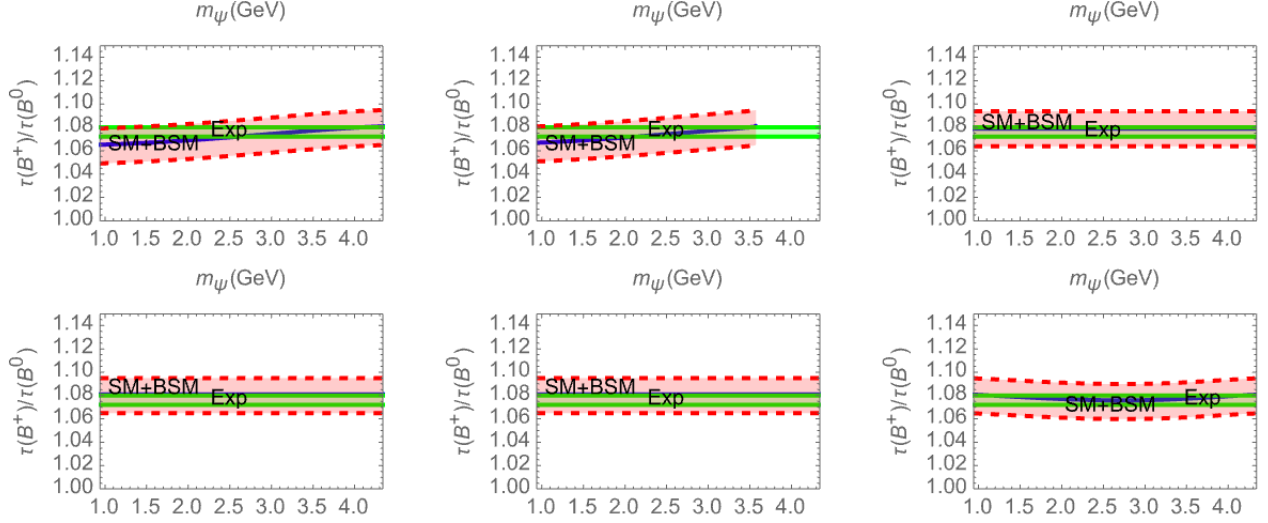


**Figure 8:** The lifetime ratio  $\tau(B^+)/\tau(B_d)$  for  $\mathcal{H}_{2/3}$  as a function of  $m_\psi$ , using the upper limits of one of the constants  $G_X^{f_1 f_2}$  and setting the others to zero. The red region shows the SM error, whereas the experimental value is shown in green. The non-vanishing constants from up to down and left to right are  $G_{IV}^{u\psi}, G_{IV}^{c\psi}, G_{IV}^{ds}, G_I^{ds}, G_I^{ss} = G_{III}^{d\psi}, G_{III}^{s\psi}$ ,

## References

- [1] G. Alonso-Álvarez, G. Elor, and M. Escudero, *Collider signals of baryogenesis and dark matter from B mesons: A roadmap to discovery*, Phys. Rev. D **104** (2021), no. 3 035028, [[arXiv:2101.02706](#)].
- [2] I. I. Balitsky, V. M. Braun, and A. V. Kolesnichenko, *Radiative Decay  $\Sigma^+ \rightarrow p\gamma$  in Quantum Chromodynamics*, Nucl. Phys. B **312** (1989) 509–550.
- [3] A. Khodjamirian, B. Melić, and Y.-M. Wang, *A guide to the QCD light-cone sum rules for b-quark decays*, Eur. Phys. J. ST **233** (2024), no. 2 271–298, [[arXiv:2311.08700](#)].
- [4] A. Khodjamirian and M. Wald, *B-meson decay into a proton and dark antibaryon from QCD light-cone sum rules*, Phys. Lett. B **834** (2022) 137434, [[arXiv:2206.11601](#)].
- [5] A. Boushmelev and M. Wald, *Higher twist corrections to B-meson decays into a proton and dark antibaryon from QCD light-cone sum rules*, Phys. Rev. D **109** (2024), no. 5 055049, [[arXiv:2311.13482](#)].
- [6] V. M. Braun, A. Lenz, N. Mahnke, and E. Stein, *Light cone sum rules for the nucleon form-factors*, Phys. Rev. D **65** (2002) 074011, [[hep-ph/0112085](#)].
- [7] A. Lenz, M. Wittmann, and E. Stein, *Improved light cone sum rules for the electromagnetic form-factors of the nucleon*, Phys. Lett. B **581** (2004) 199–206, [[hep-ph/0311082](#)].
- [8] V. M. Braun, A. Lenz, and M. Wittmann, *Nucleon Form Factors in QCD*, Phys. Rev. D **73** (2006) 094019, [[hep-ph/0604050](#)].
- [9] A. Lenz, M. Gockeler, T. Kaltenbrunner, and N. Warkentin, *The Nucleon Distribution Amplitudes and their application to nucleon form factors and the  $N \rightarrow \Delta$  transition at intermediate values of  $Q^2$* , Phys. Rev. D **79** (2009) 093007, [[arXiv:0903.1723](#)].
- [10] G. Elor and A. W. M. Guerrero, *Branching fractions of B meson decays in Mesogenesis*, JHEP **02** (2023) 100, [[arXiv:2211.10553](#)].
- [11] **RQCD** Collaboration, G. S. Bali et al., *Light-cone distribution amplitudes of octet baryons from lattice QCD*, Eur. Phys. J. A **55** (2019), no. 7 116, [[arXiv:1903.12590](#)].
- [12] Y.-J. Shi, Y. Xing, and Z.-P. Xing, *Heavy baryon decays into light meson and dark baryon within LCSR*, Eur. Phys. J. C **84** (2024), no. 3 306, [[arXiv:2401.14120](#)].
- [13] P. Ball, V. M. Braun, and E. Gardi, *Distribution Amplitudes of the  $\Lambda_b$  Baryon in QCD*, Phys. Lett. B **665** (2008) 197–204, [[arXiv:0804.2424](#)].
- [14] H.-H. Duan, Y.-L. Liu, and M.-Q. Huang, *Light-cone sum rule analysis of semileptonic decays  $A_b^0 \rightarrow A_c^+ \ell^- \bar{\nu}_\ell$* , Eur. Phys. J. C **82** (2022), no. 10 951, [[arXiv:2204.00409](#)].
- [15] Y.-J. Shi, Y. Xing, and Z.-P. Xing, *Semi-inclusive decays of B meson into a dark anti-baryon and baryons*, Eur. Phys. J. C **83** (2023), no. 8 744, [[arXiv:2305.17622](#)].
- [16] Y. Amhis et al., *Averages of b-hadron, c-hadron, and  $\tau$ -lepton properties as of 2021*, [[arXiv:2206.07501](#)].

- [17] A. Lenz, *Lifetimes and heavy quark expansion*, Int. J. Mod. Phys. A **30** (2015), no. 10 1543005, [[arXiv:1405.3601](#)].
- [18] J. Albrecht, F. Bernlochner, A. Lenz, and A. Rusov, *Lifetimes of  $b$ -hadrons and mixing of neutral  $B$ -mesons: theoretical and experimental status*, Eur. Phys. J. ST **233** (2024), no. 2 359–390, [[arXiv:2402.04224](#)].
- [19] D. King, A. Lenz, and T. Rauh,  *$SU(3)$  breaking effects in  $B$  and  $D$  meson lifetimes*, JHEP **06** (2022) 134, [[arXiv:2112.03691](#)].
- [20] D. King, A. Lenz, M. L. Piscopo, T. Rauh, A. V. Rusov, and C. Vlahos, *Revisiting Inclusive Decay Widths of Charmed Mesons*, [arXiv:2109.13219](#).
- [21] A. Lenz, M. L. Piscopo, and A. V. Rusov, *Contribution of the Darwin operator to non-leptonic decays of heavy quarks*, JHEP **12** (2020) 199, [[arXiv:2004.09527](#)].
- [22] M. L. Piscopo, *Higher order corrections to the lifetime of heavy hadrons*. PhD thesis, Siegen U., 2021. [arXiv:2112.03137](#).
- [23] T. Mannel, D. Moreno, and A. Pivovarov, *Heavy quark expansion for heavy hadron lifetimes: completing the  $1/m_b^3$  corrections*, JHEP **08** (2020) 089, [[arXiv:2004.09485](#)].
- [24] M. Kirk, A. Lenz, and T. Rauh, *Dimension-six matrix elements for meson mixing and lifetimes from sum rules*, JHEP **12** (2017) 068, [[arXiv:1711.02100](#)]. [Erratum: JHEP **06**, 162 (2020)].
- [25] A. Lenz and T. Rauh,  *$D$ -meson lifetimes within the heavy quark expansion*, Phys. Rev. **D88** (2013) 034004, [[arXiv:1305.3588](#)].
- [26] F. Gabbiani, A. I. Onishchenko, and A. A. Petrov, *Spectator effects and lifetimes of heavy hadrons*, Phys. Rev. **D70** (2004) 094031, [[hep-ph/0407004](#)].
- [27] E. Franco, V. Lubicz, F. Mescia, and C. Tarantino, *Lifetime ratios of beauty hadrons at the next-to-leading order in QCD*, Nucl. Phys. **B633** (2002) 212–236, [[hep-ph/0203089](#)].
- [28] M. Beneke, G. Buchalla, C. Greub, A. Lenz, and U. Nierste, *The  $B^+ - B_d^0$  Lifetime Difference Beyond Leading Logarithms*, Nucl. Phys. **B639** (2002) 389–407, [[hep-ph/0202106](#)].
- [29] A. Lenz, M. L. Piscopo, and A. V. Rusov, *Disintegration of beauty: a precision study*, JHEP **01** (2023) 004, [[arXiv:2208.02643](#)].
- [30] M. Black, M. Lang, A. Lenz, and Z. Wüthrich, *HQET sum rules for matrix elements of dimension-six four-quark operators for meson lifetimes within and beyond the Standard Model*, [arXiv:2412.13270](#).
- [31] M. Egner, M. Fael, A. Lenz, M. L. Piscopo, A. V. Rusov, K. Schönwald, and M. Steinhauser, *Total decay rates of  $B$  mesons at NNLO-QCD*, [arXiv:2412.14035](#).
- [32] **HPQCD** Collaboration, C. T. H. Davies, J. Harrison, G. P. Lepage, C. J. Monahan, J. Shigemitsu, and M. Wingate, *Lattice QCD matrix elements for the  $B_s^0 - \bar{B}_s^0$  width difference beyond leading order*, Phys. Rev. Lett. **124** (2020), no. 8 082001, [[arXiv:1910.00970](#)].
- [33] R. J. Dowdall, C. T. H. Davies, R. R. Horgan, G. P. Lepage, C. J. Monahan, J. Shigemitsu, and M. Wingate, *Neutral  $B$ -meson mixing from full lattice QCD at the physical point*, Phys. Rev. D **100** (2019), no. 9 094508, [[arXiv:1907.01025](#)].

- [34] **Fermilab Lattice, MILC Collaboration**, A. Bazavov et al.,  $B_{(s)}^0$ -mixing matrix elements from lattice QCD for the Standard Model and beyond, Phys. Rev. D **93** (2016), no. 11 113016, [[arXiv:1602.03560](#)].
- [35] L. Di Luzio, M. Kirk, A. Lenz, and T. Rauh,  $\Delta M_s$  theory precision confronts flavour anomalies, JHEP **12** (2019) 009, [[arXiv:1909.11087](#)].
- [36] D. King, A. Lenz, and T. Rauh,  $B_s$  mixing observables and  $|V_{td}/V_{ts}|$  from sum rules, JHEP **05** (2019) 034, [[arXiv:1904.00940](#)].
- [37] A. G. Grozin, R. Klein, T. Mannel, and A. A. Pivovarov,  $B^0 - \bar{B}^0$  mixing at next-to-leading order, Phys. Rev. D **94** (2016), no. 3 034024, [[arXiv:1606.06054](#)].
- [38] A. Lenz and U. Nierste, *Theoretical update of  $B_s - \bar{B}_s$  mixing*, JHEP **06** (2007) 072, [[hep-ph/0612167](#)].
- [39] M. Beneke, G. Buchalla, A. Lenz, and U. Nierste, *CP asymmetry in flavor specific B decays beyond leading logarithms*, Phys. Lett. B **576** (2003) 173–183, [[hep-ph/0307344](#)].
- [40] M. Beneke, G. Buchalla, C. Greub, A. Lenz, and U. Nierste, *Next-to-leading order QCD corrections to the lifetime difference of  $B_s$  mesons*, Phys. Lett. B **459** (1999) 631–640, [[hep-ph/9808385](#)].
- [41] M. Beneke, G. Buchalla, and I. Dunietz, *Width Difference in the  $B_s - \bar{B}_s$  System*, Phys. Rev. D **54** (1996) 4419–4431, [[hep-ph/9605259](#)]. [Erratum: Phys.Rev.D 83, 119902 (2011)].
- [42] A. S. Dighe, T. Hurth, C. S. Kim, and T. Yoshikawa, *Measurement of the lifetime difference of  $B_d$  mesons: Possible and worthwhile?*, Nucl. Phys. B **624** (2002) 377–404, [[hep-ph/0109088](#)].
- [43] C. Miró, M. Escudero, and M. Nebot, *How large could CP violation in neutral B meson mixing be? Implications for baryogenesis and upcoming searches*, [arXiv:2410.13936](#).
- [44] G. Elor, M. Escudero, and A. Nelson, *Baryogenesis and Dark Matter from B Mesons*, Phys. Rev. D **99** (2019), no. 3 035031, [[arXiv:1810.00880](#)].
- [45] **Particle Data Group Collaboration**, P. A. Zyla et al., *Review of Particle Physics*, PTEP **2020** (2020), no. 8 083C01.
- [46] **BaBar Collaboration**, J. P. Lees et al., *Search for Evidence of Baryogenesis and Dark Matter in  $B^+ \rightarrow \psi_D + p$  Decays at BABAR*, Phys. Rev. Lett. **131** (2023), no. 20 201801, [[arXiv:2306.08490](#)].